PCCP

Accepted Manuscript

ROYAL SOCIETY OF CHEMISTRY

www.rsc.org/pccp

PCCP

RSCPublishing

ARTICLE

Aromatic-Hydroxyl Interaction of an alpha-aryl ether Lignin Model-Compound on SBA-15, Present at Pyrolysis Temperatures

M. V. Kandziolka,[b] M. K. Kidder,[b] L. Gill,[b] Z. Wu,[c] and A. Savara[a*]

Cite this: DOI: 10.1039/x0xx00000x

Received ooth January 2014,
Accepted ooth January 2014

DOI: 10.1039/x0xx00000x

www.rsc.org/

An aromatic alpha-aryl ether compound (a benzyl phenyl ether analogue) was covalently grafted to mesoporous silica SBA-15, to create BPEa-SBA-15. The BPEa-SBA-15 was subjected to successive heating cycles up to 600 °C, with in situ monitoring by DRIFTS. It was found that the toluene moiety coordinates to SBA-15 surface silanol hydroxyl groups via an aromatic-hydroxyl interaction. This interaction is evidenced by a red-shift of the aromatic C-H stretches, as well as a red-shift and broadening of the surface hydroxyl O-H stretches, which are features characteristic of a hydrogen bond. These features remain present during heating until ~400 °C whereupon the ether linkage of BPEa-SBA-15 is cleaved, accompanied by loss of the toluene moiety.

Introduction

Hydrogen bonds span a wide range of bond strengths,[1-4] are defined by interaction between a proton and an atom or group of atoms with evidence of a bond,[3-5] and can be involved in determining the structures of molecules and crystals when they are present.[4, 6] Here, we present evidence of a hydrogen bond based aromatic-hydroxyl interaction with an α-aryl ether moiety in a lignin model compound on a porous silicate. The aromatic-hydroxyl interaction presented here is conceptually similar to cation-π interactions, which are known to be determining factors in the structure of macromolecules.[7] Hydrogen bonds can have an orienting effect even when they are not the dominant interaction, and such orienting effects from hydrogen bonds have recently received great attention for their ability to control the product selectivities in catalytic reactions.[8-12] Here, we sought to understand the interactions that a lignin model compound might have with a silicate surface as silicate materials are used in the pyrolysis of biomass such as a lignin. Interestingly and surprisingly, in this study an aromatic-hydroxyl interaction is detected for an α-aryl ether compound on SBA-15, a porous silicate material, and the aromatic-hydroxyl interaction is present even at ~400 °C (pyrolysis temperatures).

The utilization of biomass derived lignin as a renewable source of fuels or platform chemicals is a topic of current societal interest, and includes conversions of α-aryl ether linkages during pyrolysis. Among the methods currently being considered are a) pyrolysis followed by heterogeneous catalytic conversion of the pyrolysis vapors, and b) catalytic fast pyrolysis. In the first option, uncatalyzed pyrolysis of lignin produces a variety of chemicals including lignin monomers and oligomers which may be further broken down via heterogeneous catalysis, which typically employs metal oxide-based catalysts and/or supports (e.g., MCM-41, SBA-15, zeolites).[13-18] In the second option (catalytic fast pyrolysis), lignin is pyrolyzed in the presence of a solid catalyst, and the solid typically has acidic surface hydroxyl groups which play a role in the catalytic conversion of the lignin.[17, 19-22] The interaction of lignin chemical moieties with surface hydroxyls may be important for catalytic fast pyrolysis lignin conversions, and potentially other heterogeneous catalysis based lignin conversions. Other groups have studied the chemistry and interactions of biomass derivatives with catalytically active surfaces.[23-26] In this study, we do not investigate lignin conversions and instead conduct a model compound study on the interactions of an α-aryl ether compound with a silicate surface - specifically, the surface hydroxyl groups of SBA-15 - using infrared spectroscopy. We find that there is an aromatic-hydroxyl interaction that persists at elevated temperatures (up to 400 °C). The possibility of an aromatic-hydroxyl interaction in such chemical systems, particularly at such high temperatures, is currently not well appreciated in the field.

Benzyl phenyl ether (BPE) serves as a model compound for studying the chemistry of lignin α-aryl ether linkages.[27] In this study, we used a BPE analogue (BPEa) as the reactant, by covalently grafting meta-$HOC_6H_4OCH_2C_6H_5$ to SBA-15 to produce BPEa-SBA-15, shown in Fig. 1. The individual BPEa

species are less than half the diameter of the pores in SBA-15. For clarity and simplicity, we will refer to the two halves of the BPEa molecule as the toluene moiety and the phenoxy moiety.

We show evidence that there is an aromatic-hydroxyl interaction between the BPEa toluene moiety and SBA-15 surface hydroxyls (Fig. 1). The aromatic-hydroxyl interaction is observed to be present during heating, until the α-carbon-ether linkage breaks. This aromatic-hydroxyl interaction is present at temperatures up to ~400 °C and thus should be present during catalytic fast pyrolysis processes and other catalytic processes which involve lignin: there may be kinetic / mechanistic implications for catalytic pyrolysis. We focus on the chemistry and the infrared redshifts associated with the aromatic-hydroxyl interaction, with supporting evidence from other analytical techniques provided in the supporting information.

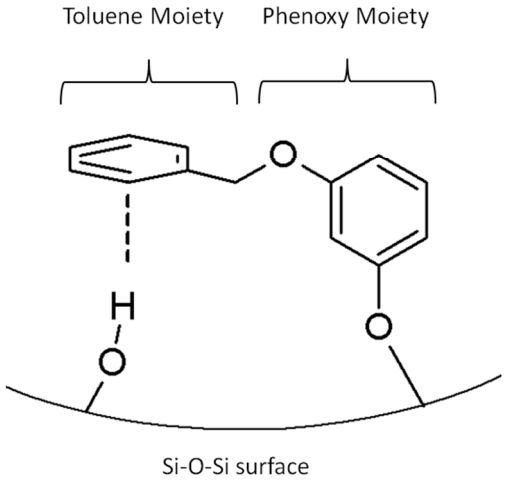

Fig. 1. Depiction of BPEa-SBA-15, with the toluene moiety interacting with a nearby SBA-15 surface hydroxyl

Results and Discussion

The BPEa-SBA15 was heated and monitored by *in situ* DRIFTS spectroscopy as described in the experimental section. In these experiments, infrared peaks are proportional to the concentration of the adsorbates. Fig. 2 shows the DRIFTS spectra of the C-H stretching region (~2800-3200 cm^{-1}), and the C-C ring stretching region (~1600 cm^{-1}) obtained from successive heatings of BPEa-SBA-15. C-H stretching changes are observed in both Region I and Region II in Fig. 2, spanning approximately 3100-3000 cm^{-1} and 3000-2800 cm^{-1}.

After heating to 300 °C the intensity of C-H region II decreases, as does the aromatic C-C ring stretching band at ~1600 cm^{-1}. This is consistent with mass spectrometry data and thermogravimetric analysis data in sections S3 and S4 of the supporting information. Thermogravimetric analysis (TGA) shows that by 300 °C only a minority of the grafted BPEa has decomposed, while mass spectrometry shows that toluene is the primary organic product and that most of the adsorbed water has left the sample before 300 °C. Upon further heating to 600 °C, the aromatic C-C ring stretching bands at ~1600 cm^{-1} in Fig. 2 decrease by approximately 50%, which is attributed to removal of the toluene moiety without removal of the phenoxy moiety, based on the mass spectrometry data and ^{13}C NMR data in sections S3 and S6 of the supporting information.

The above data enable us to conclude that when heating to 600 °C, the primary reaction is cleavage at the ether bond with removal of the toluene half of the molecule, consistent with previous experiments[27] and further analysis of the infrared spectra (below). Interestingly, as seen in Fig. 2, upon cleavage of the ether bond and upon loss of the toluene moiety, there is virtually no change in C-H Region I (the "normal position" of aromatic C-H stretches) while there is nearly a total loss of

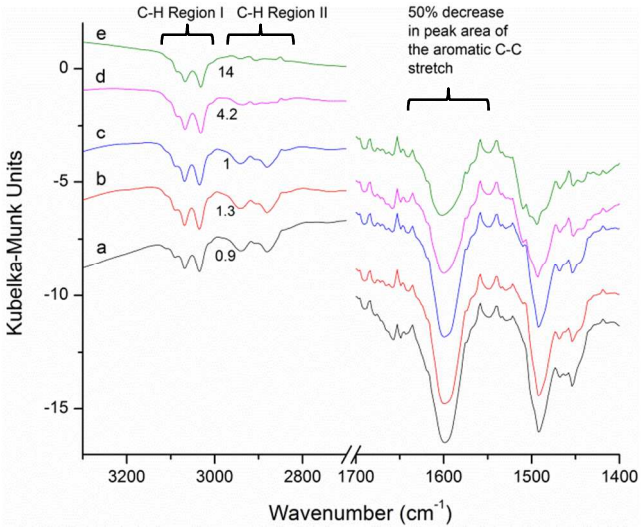

Fig. 2. DRIFTS spectra of BPEa-SBA-15 in the C-H stretching region and aromatic C-C ring stretching region at (a) 70 °C before heating, as well as at 70 °C after heating to (b) 300 °C, (c) 350 °C, (d) 400 °C, and (e) 600 °C. Spectra have been vertically translated for clarity.

intensity in C-H region II (the normal position of alkyl C-H stretches). How is it possible for the toluene half of the molecule to leave without any appreciable loss of intensity in C-H region I? As will be explained, this situation arises because the aromatic ring of the toluene moiety interacts with surface hydroxyls, and this aromatic-hydroxyl interaction shifts the majority of the intensity associated with the aromatic C-H stretches of the toluene moiety into the frequency range of C-H Region II. For the spectra of bulk BPE and gas phase BPE, the ratios of the peak areas of C-H region I to C-H region II are ~2.0 and >4.0, respectively (see Supporting Information). As is evident from Fig. 2 spectrum a, for BPEa-SBA-15, the ratio of the peak area of C-H region I to C-H region II is <1.0 in the initial spectrum at 70 °C, which is very different from pure BPE.

Fig. 3 shows the difference spectra of BPEa-SBA-15, indicative of the species which have left during heating to each temperature. Effectively, Fig. 3 shows spectra where the peaks correspond primarily to the removed toluene moiety, enabling

the C-H Region I to C-H Region II ratio to be visually compared to literature data.[28-30] As shown in Spectra a through c of Fig. 3, there is minimal intensity associated with the toluene moiety of BPEa-SBA-15 in C-H region I, while most of the C-H stretching intensity associated with the toluene moiety of BPEa-SBA-15 is present in C-H region II.

Evidently, the aromatic C-H stretches of the toluene moiety have "disappeared" or have shifted in frequency from C-H Region I to C-H Region II after heating BPEa-SBA-15. We invoke the latter explanation, and will elaborate. First, solid state NMR data (shown in the supporting information) indicates that the BPEa species has not decomposed during grafting, and the toluene moiety is still a toluene moiety as shown in Fig. 1. There is no physical reason to expect the C-H stretches to "disappear" from interaction with the surface -- regardless of orientation -- when BPEa is grafted to an insulating oxide (i.e., there are no surface selection rules which could explain the data).

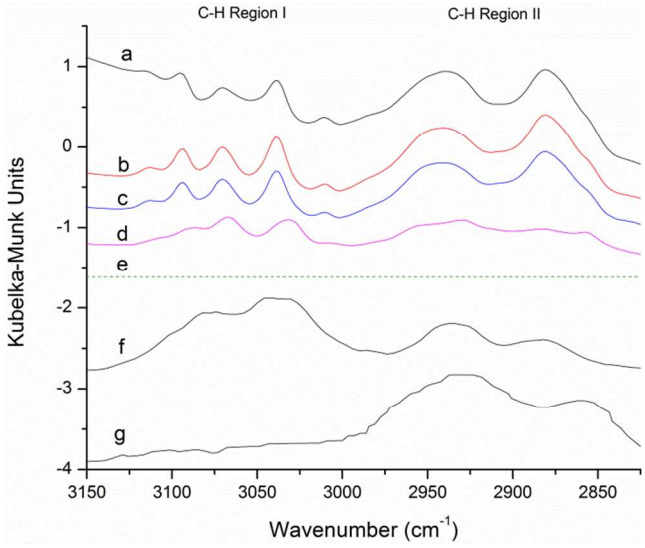

Fig. 3. DRIFTS difference spectra of BPEa-SBA-15 in the C-H stretching region, effectively showing the peaks associated with the toluene intensity. Spectra were obtained by taking the spectrum after the final heating (600 °C) minus the spectrum obtained for (a) 70 °C before heating, as well as at 70 °C after heating to (b) 300 °C, (c) 350 °C, (d) 400 °C, and (e) 600 °C. Spectrum (f) is of gas phase toluene (NIST reference) and (g) is of toluene on SBA-15 from Mirji *et al*.[28] Spectra have been vertically translated for clarity.

Further, this interpretation of the peaks associated with the toluene moiety are consistent with previous data in the literature. Spectrum g in Fig. 3 was taken for toluene adsorbed on SBA-15 by Mirji *et al*.[28] Note that the same behavior is observed for toluene on SBA-15: a lack of intensity in C-H Region I, and only intensity in C-H Region II. Similarly, Trombetta *et. al*.[29] studied the interaction of several aromatic compounds with the hydroxyl groups of H-ZSM-5 zeolites, and their study included infrared measurements. In the study by Trombetta *et. al.*, visual inspection of the infrared spectra of toluene and xylenes on H-ZSM-5 clearly shows that there is a lack of intensity in C-H Region I relative to C-H Region II (when compared to either liquid or gas phase molecules). Though not appreciated by the authors of the previous studies, their data is consistent with our interpretation that such aromatic-hydroxyl interactions cause a frequency redshift for the aromatic C-H stretches. Aromatic C-H frequency[30] redshifts have also been observed in organometallic compounds, such as $W(C_6H_6)_2$ and $V(C_6H_6)$. The existence of the aromatic-hydroxyl interaction is even more clearly evident after analysis of the hydroxyl region in our infrared spectra, as described below.

The hydroxyl region of the same BPEa-SBA-15 infrared spectra are shown in Fig. 4, along with the spectra for neat SBA-15 before heating and after heating to 600 °C. The sharp peak at 3745 cm^{-1} corresponds to the OH vibrations of free hydroxyls on SBA-15, as is evident by the presence of this peak in neat SBA-15 after heating to 600 °C.

Upon covalent grafting of BPEa onto SBA-15 the peak associated with the isolated hydroxyl is virtually completely removed (spectra a and b of Fig. 4) and broad hydroxyl peaks with greater intensity concurrently appear at lower wavenumbers. Spectrum a of Fig. 4 is before the temperature ramp and some water is still present at this temperature. Spectrum a of Fig. 4 includes a broad peak at ~3400 cm^{-1}, associated with O-H stretches of surface hydroxyl groups that are hydrogen bonded to water molecules, as well as O-H stretches within the water molecules that are hydrogen bonded to each other and surface hydroxyls (compare to spectrum f, which is for neat SBA-15 with some adsorbed water).

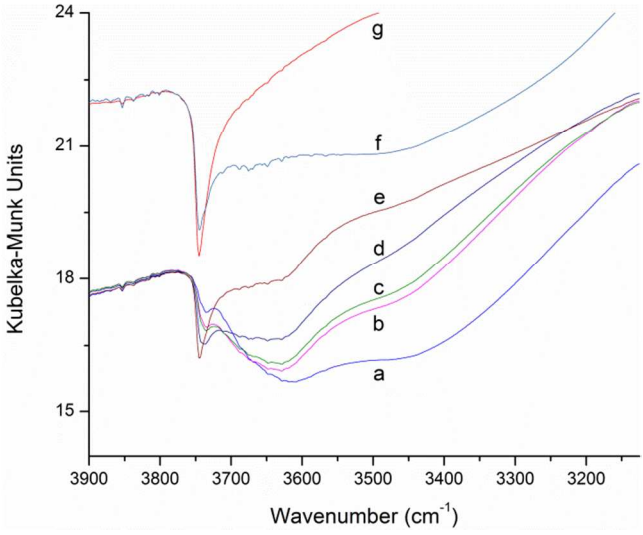

Fig. 4. DRIFTS spectra of BPEa-SBA-15 in the OH stretching region at (a) 70 °C before heating, as well as at 70 °C after heating to (b) 300 °C, (c) 350 °C, (d) 400 °C, (e) 600 °C. For comparison, DRIFTS spectra of neat SBA-15 are shown for both (f) before heating and (g) after heating to 600 °C. Spectra have been vertically translated for clarity.

As mentioned previously, by heating to 300 °C the water is removed, and in spectrum b of Fig. 4 we see that the broad

hydroxyl peaks remain redshifted to much lower wavenumbers, and with much greater intensity relative to the isolated hydroxyls. There are two broad and intense infrared absorption peaks, which are associated with the coordinated hydroxyls present in BPEa-SBA-15: one peak at ~3450 cm^{-1} and one at ~3610 cm^{-1} (these peaks will be discussed more below). The redshift observed for the new hydroxyl stretches and the increased intensity (which implies an increase of the infrared absorption cross-section) are both characteristic spectroscopic features of hydrogen bonding,[5] and are indicative of the interaction between the toluene moiety and silanol. In general, the interaction between surface hydroxyls and electron-donating adsorbates leads to a shift of the sharp free hydroxyl band to lower wavenumbers.[31-35] The strength of the aromatic-hydroxyl interaction with the toluene moiety is reflected in the degree of the redshift in wavenumbers of the hydroxyl infrared absorption band (discussed in section S9 of the supporting information).[33] Similar hydroxyl redshifts have been observed when anisole and phenol molecules hydrogen bond with hydroxyls on oxide surfaces: whether through the aromatic ring, the organic molecule's oxygen, or the alcohol hydrogen.[23]

After heating to 600 °C (spectrum e in Fig. 4), the toluene moiety has been removed, and a hydroxyl band is observed at ~3650 cm^{-1}, which we assign to the hydroxyl on the aromatic ring of grafted phenol,[36] the co-product produced after breakage of the BPEa-SBA-15 ether bond. Note that after the toluene moiety has been removed, ~50% of the free hydroxyls (~3745 cm^{-1}) are recovered relative to spectrum g (peak integration parameters are provided in section S5 of the supporting information). This ratio is consistent with a stoichiometric picture where (during grafting) ~50% of the free hydroxyls were replaced by BPEa, while ~50% of the hydroxyls were coordinated with the toluene moiety of BPEa. Quantitative analysis of the TGA data in section S4 of the supporting information is consistent with the above interpretation: the total weight loss by 600° C is 9%, and the calculated upper limit for initial weight contribution from the toluene moieties is 9.7%. For comparison, if the full BPEa species was lost, the calculated weight loss upper limit would be is 21.0 %.

Fig. 5 shows scaled peak areas for the peaks associated with the various chemical moieties we have discussed above, as a function of heating. The stoichiometry of these changes follows the interpretation above: The coordinated hydroxyls associated with the aromatic-hydroxyl interaction decrease concomitantly with the appearance of the free hydroxyls with remarkable agreement (the white circles and black circles in Fig. 5). These changes are also concomitant with the decrease of intensity of C-H Region II and in the aromatic C-C ring stretching region. These stoichiometric changes are clear evidence that as the toluene moiety of BPEa-SBA-15 leaves, the SBA-15 surface hydroxyls return to their free hydroxyl state, indicating that the toluene moiety is coordinated with SBA-15 surface silanols prior to decomposition of the grafted BPEa.

We note that although the aromatic-hydroxyl interaction in this study is present to ~400°C, the aromatic-hydroxyl interaction may not be the dominant interaction, but may simply be "orienting" the toluene ring of the BPEa molecule. In the present study the molecule is tethered, and for a molecule of this size, the van der Waal's interactions for physisorption[37, 38] are likely strong enough to be more dominant than the aromatic-hydroxyl interaction. However, the presence of the aromatic-hydroxyl interaction is not due to the orientation being confined by tethering: even BPE physisorbed on SBA-15 shows the same infrared spectral pattern and NMR evidence of hydrogen bonding (spectra provided in Section S8 of the Supporting Information), and the other literature examples explained by our interpretation were also physisorbed. Thus, our results and the literature suggest that the aromatic-hydroxyl interaction may be orienting even when it is not dominant. The aromatic-hydroxyl interaction may even be 'breaking and reforming', with the molecule spending more time in the coordinated configuration than in the on the coordinated configuration for the temperature range monitored in our experiments (resulting in the coordinated configuration being detected by infrared spectroscopy).

The large molecular weight of lignin polymers should inhibit lignin desorption, enabling aromatic groups to remain in the proximity of the surface hydroxyls of solid acid catalysts even at elevated temperatures. These aromatic-hydroxyl interactions should thus be expected to be present during catalytic fast pyrolysis and other heterogenous catalysis transformations of lignin-type oligomers. With further research, it is possible that aromatic-hydroxyl interactions may even be tailored to increase the rates or selectivities in thermocatalytic lignin decomposition processes. Further study of aromatic-hydroxyl interactions may be necessary for developing accurate kinetic and mechanistic models of the catalytic fast pyrolysis mechanism of lignin,[39] as is currently being done for cellulose.[40, 41]

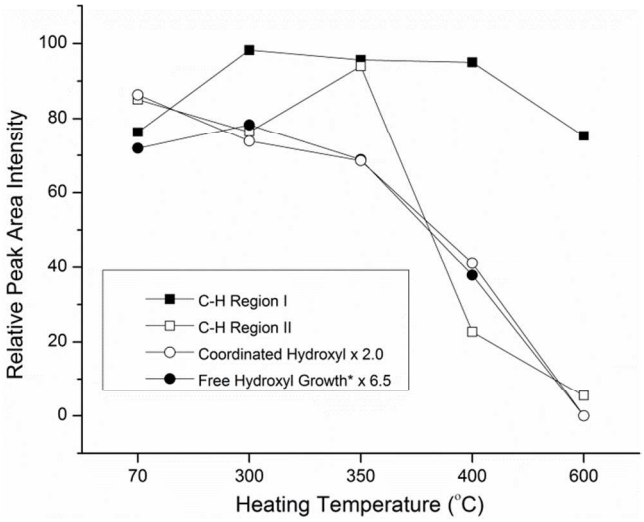

Fig. 5. Peak area intensities of various regions of the DRIFTS spectrum of BPEa-SBA-15 at (1) 70 °C before heating, and 70 °C after heating to (2) 300 °C, (3) 350 °C, (4) 400 °C, and (5), 600 °C. Peak areas scaled for comparison with scaling factors shown in legend. *The free hydroxyl data is plotted as 'final minus initial' to enable direct comparison to the coordinated hydroxyl data.

Experimental Section

BPEa-SBA-15 was prepared by covalently grafting meta-$HOC_6H_4OCH_2C_6H_5$ to SBA-15 by heating at 200 °C based on a grafting procedure used previously.[27].Literature procedures were used to synthesize meta-$HOC_6H_4OCH_2C_6H_5$[42] and SBA-15[43]. The organic template was removed by combustion – the temperature was ramped at 10C/min up to 550 °C and held there for 6 hours in an air stream before cooling down. BPEa was grafted subsequent to removal of the organic template. The grafting coverage of BPEa-SBA-15 was determined to be 1.05 mmol BPEa per gram by dissolution of the silicate material using 1M NaOH followed by chemical analysis as described elsewhere.[44] Subsequent to preparation, BPEa-SBA-15 was kept in an evacuated desiccator to prevent large quantities of water adsorption, though small quantities of water still adsorbed from ambient air during sample transfers. Fortunately, water desorbs from the sample prior to the temperature range of interest, as described in the results and discussion section.

Flow pyrolysis experiments were run in an HC-900 Pike Technologies DRIFTS cell with a Helium flow of 25 mL per minute, the cell was successively heated to temperatures ranging from 300 °C to 600 °C with a heating rate of 5 °C per minute and then cooled to 70 °C between each heating. During heating, mass spectrometry data was obtained from a capillary in the effluent using an Omnistar GSD-301 O2 Pfeiffer Vacuum mass spectrometer. DRIFTS spectra were obtained at a spectral resolution of 4 cm^{-1} using a Nicolet Nexus 670 FTIR spectrometer with an MCT/A detector. The infrared spectrometer software (OMNIC) automatically applied the Kubelka-Munk transformation, providing the signal intensity in Kubelka-Munk units which are proportional to absorbance for many DRIFTS measurements[45] and are quantitative for comparing changes in an adsorbate intensity on a single sample, or comparing the ratio between peaks of a single sample.[46] DRIFTS generally cannot be used for quantitative comparisons of adsorbate concentrations between different samples,[47] and there are cases when absorbance units are more linear with adsorbate concentration relative to Kubelka-Munk units.[48] The stoichiometric consistency displayed in Fig. 5 indicates that Kubelka-Munk units are sufficiently linear with adsorbate concentration in our experiments. DRIFTS spectra were obtained before during and after each heating: no qualitative changes were observed between the spectra of the latter two cases. Infrared peak integrations were performed using linear baselines, with the baselines and regions used provided in the supporting information.

Conclusions

There is an aromatic-hydroxyl interaction between the toluene moieties of covalently grafted BPEa and SBA-15 hydroxyls. In BPEa-SBA-15 the aromatic-hydroxyl interaction is present even with water adsorbed from the ambient air, and is present up to ~400°C under a helium flow, whereupon the α-ether linkage is thermally cleaved and the toluene moiety desorbs. Aromatic-hydroxyl interactions are thus expected to be present during conversions of lignin pyrolysis products and catalytic fast pyrolysis of lignin, and may need to be considered for accurate kinetic and mechanistic models of catalytic fast pyrolysis of lignin.

Acknowledgements

This research was sponsored by the Division of Chemical Sciences, Geosciences, and Biosciences, Office of Basic Energy Sciences, U.S. Department of Energy. A portion of this research (in situ IR spectroscopy) was conducted at the Center for Nanophase Materials Sciences, which is sponsored at Oak Ridge National Laboratory by the Scientific User Facilities Division, Office of Basic Energy Sciences, U.S. Department of Energy.

Notes and references

[a] Chemical Sciences Division, Oak Ridge National Laboratory, Oak Ridge, Tennessee, 37831. savaraa@ornl.gov

[b] Chemical Sciences Division, Oak Ridge National Laboratory, Oak Ridge, Tennessee, 37831.

[c] Address here. Chemical Sciences Division, and Center for Nanophase Materials Sciences, Oak Ridge National Laboratory, Oak Ridge, Tennessee, 37831

Electronic Supplementary Information (ESI) available: IR peak integration details, mass spectrometry data, thermogravimetric analysis data, NMR data, and discussion about the strength of the aromatic-hydroxyl bond. See DOI: 10.1039/b000000x/

1. I. Mata, I. Alkorta, E. Molins and E. Espinosa, *Chem-Eur J*, 2010, **16**, 2442-2452.
2. P. Gilli, L. Pretto, V. Bertolasi and G. Gilli, *Accounts Chem Res*, 2009, **42**, 33-44.
3. T. Steiner, *Angew Chem Int Edit*, 2002, **41**, 48-76.
4. G. R. Desiraju, *Angew Chem Int Edit*, 2011, **50**, 52-59.
5. E. Arunan, G. R. Desiraju, R. A. Klein, J. Sadlej, S. Scheiner, I. Alkorta, D. C. Clary, R. H. Crabtree, J. J. Dannenberg, P. Hobza, H. G. Kjaergaard, A. C. Legon, B. Mennucci and D. J. Nesbitt, *Pure Appl Chem*, 2011, **83**, 1637-1641.
6. J. Bernstein, R. E. Davis, L. Shimoni and N.-L. Chang, *Angewandte Chemie International Edition in English*, 1995, **34**, 1555-1573.
7. A. S. Mahadevi and G. N. Sastry, *Chem Rev*, 2013, **113**, 2100-2138.
8. M. S. Taylor and E. N. Jacobsen, *Angew Chem Int Edit*, 2006, **45**, 1520-1543.
9. S. Das, C. D. Incarvito, R. H. Crabtree and G. W. Brudvig, *Science*, 2006, **312**, 1941-1943.
10. G. Rivera and R. H. Crabtree, *J Mol Catal a-Chem*, 2004, **222**, 59-73.
11. P. M. Pihko, *Angew Chem Int Edit*, 2004, **43**, 2062-2064.
12. C. C. J. Loh and D. Enders, *Chemistry – A European Journal*, 2012, **18**, 10212-10225.
13. J. Adam, E. Antonakou, A. Lappas, M. Stocker, M. H. Nilsen, A. Bouzga, J. E. Hustad and G. Oye, *Micropor Mesopor Mat*, 2006, **96**, 93-101.

14. Y. Zhao, L. Deng, B. Liao, Y. Fu and Q. X. Guo, *Energ Fuel*, 2010, **24**, 5735-5740.
15. Q. Lu, X. F. Zhu, W. Z. Li, Y. Zhang and D. Y. Chen, *Chinese Sci Bull*, 2009, **54**, 1941-1948.
16. Z. Tang, Y. Zhang and Q. X. Guo, *Ind Eng Chem Res*, 2010, **49**, 2040-2046.
17. V. M. Roberts, V. Stein, T. Reiner, A. Lemonidou, X. B. Li and J. A. Lercher, *Chem-Eur J*, 2011, **17**, 5939-5948.
18. A. Savara, A. Danon, W. M. H. Sachtler and E. Weitz, *Phys Chem Chem Phys*, 2009, **11**, 1180-1188.
19. G. W. Huber, S. Iborra and A. Corma, *Chem Rev*, 2006, **106**, 4044-4098.
20. T. P. Vispute, H. Y. Zhang, A. Sanna, R. Xiao and G. W. Huber, *Science*, 2010, **330**, 1222-1227.
21. H. W. Lee, T. H. Kim, S. H. Park, J. K. Jeon, D. J. Suh and Y. K. Park, *J Nanosci Nanotechno*, 2013, **13**, 2640-2646.
22. A. L. Marshall and P. J. Alaimo, *Chem-Eur J*, 2010, **16**, 4970-4980.
23. A. Popov, E. Kondratieva, J. M. Goupil, L. Mariey, P. Bazin, J.-P. Gilson, A. Travert and F. Maugé, *The Journal of Physical Chemistry C*, 2010, **114**, 15661-15670.
24. A. Popov, E. Kondratieva, L. Mariey, J. M. Goupil, J. El Fallah, J.-P. Gilson, A. Travert and F. Maugé, *J Catal*, 2013, **297**, 176-186.
25. J. R. Copeland, I. A. Santillan, S. M. Schimming, J. L. Ewbank and C. Sievers, *J Phys Chem C*, 2013, **117**, 21413-21425.
26. C. Lucarelli, A. Giugni, G. Moroso and A. Vaccari, *The Journal of Physical Chemistry C*, 2012, **116**, 21308-21317.
27. M. K. Kidder, P. F. Britt and A. C. Buchanan, *Energ Fuel*, 2006, **20**, 54-60.
28. S. A. Mirji, S. B. Halligudi, D. P. Sawant, K. R. Patil, A. B. Gaikwad and S. D. Pradhan, *Colloid Surface A*, 2006, **272**, 220-226.
29. M. Trombetta, T. Armaroli, A. G. Alejandre, J. R. Solis and G. Busca, *Appl Catal a-Gen*, 2000, **192**, 125-136.
30. K. Nakamoto, *Infrared and Raman Spectra of Inorganic and Coordination Compounds: Applications in coordination, organometallic, and bioinorganic chemistry*, Wiley, 1997.
31. J. H. Anderson, J. Lombardi and M. L. Hair, *J Colloid Interf Sci*, 1975, **50**, 519-524.
32. D. M. Haaland, *Surf Sci*, 1981, **102**, 405-423.
33. W. Pohle, *J Chem Soc Farad T 1*, 1982, **78**, 2101-2109.
34. M. B. Sayed and R. P. Cooney, *J Colloid Interf Sci*, 1983, **91**, 552-559.
35. K. Chakarova and K. Hadjiivanov, *Micropor Mesopor Mat*, 2011, **143**, 180-188.
36. E. P.J. Linstrom and W.G. Mallard, National Institute of Standards and Technology, Gaithersburg MD, 20899.
37. W. Liu, A. Savara, X. G. Ren, W. Ludwig, K. H. Dostert, S. Schauermann, A. Tkatchenko, H. J. Freund and M. Scheffler, *J Phys Chem Lett*, 2012, **3**, 582-586.
38. A. Savara, C. M. Schmidt, F. M. Geiger and E. Weitz, *J Phys Chem C*, 2009, **113**, 2806-2815.
39. R. N. Olcese, J. Francois, M. M. Bettahar, D. Petitjean and A. Dufour, *Energ Fuel*, 2013, **27**, 975-984.
40. H. B. Mayes and L. J. Broadbelt, *J Phys Chem A*, 2012, **116**, 7098-7106.
41. R. Vinu and L. J. Broadbelt, *Energ Environ Sci*, 2012, **5**, 9808-9826.
42. A. C. Buchanan, P. F. Britt, J. T. Skeen, J. A. Struss and C. L. Elam, *J Org Chem*, 1998, **63**, 9895-9903.
43. J. Jarupatrakorn and J. D. Tilley, *J Am Chem Soc*, 2002, **124**, 8380-8388.
44. M. K. Kidder, P. F. Britt, Z. T. Zhang, S. Dai, E. W. Hagaman, A. L. Chaffee and A. C. Buchanan, *J Am Chem Soc*, 2005, **127**, 6353-6360.
45. S. R. Culler, in *Practical Techniques for Infrared Analysis*, ed. P. B. Coleman, CRC Press, Boca Raton, Florida., 1993.
46. A. Savara and E. Weitz, *Annual Review of Physical Chemistry*, 2014, **65**, 249-273.
47. F. Boroumand, H. Vandenbergh and J. E. Moser, *Anal Chem*, 1994, **66**, 2260-2266.
48. J. Sirita, S. Phanichphant and F. C. Meunier, *Anal Chem*, 2007, **79**, 3912-3918.